Chemical Research in Toxicology

Article

pubs.acs.org/crt

Interception of Benzo[*a*]pyrene-7,8-dione by UDP Glucuronosyltransferases (UGTs) in Human Lung Cells

Li Zhang,[†] Meng Huang,[†] Ian A. Blair,[†,‡] and Trevor M. Penning*[,†,‡]

[†]Center of Excellence in Environmental Toxicology and [‡]Center for Cancer Pharmacology, Department of Pharmacology, Perelman School of Medicine, University of Pennsylvania, Philadelphia, Pennsylvania 19104-6160, United States

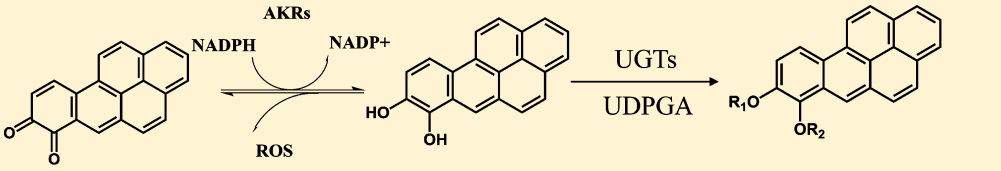

B[*a*]P-7,8-dione Catechol Catechol conjugates

R_1, R_2=H or Glucuronic acid

ABSTRACT: Polycyclic aromatic hydrocarbons (PAHs) are environmental and tobacco carcinogens. Proximate carcinogenic PAH *trans*-dihydrodiols are activated by human aldo-keto reductases (AKRs) to yield electrophilic and redox-active *o*-quinones. Interconversion among benzo[*a*]pyrene (B[*a*]P)-7,8-dione, a representative PAH *o*-quinone, and its corresponding catechol generates a futile redox-cycle with the concomitant production of reactive oxygen species (ROS). We investigated whether glucuronidation of B[*a*]P-7,8-catechol by human UDP glucuronosyltransferases (UGTs) could intercept the catechol in three different human lung cells. RT-PCR showed that UGT1A1, 1A3, and 2B7 were only expressed in human lung adenocarcinoma A549 cells. The corresponding recombinant UGTs were examined for their kinetic constants and product profile using B[*a*]P-7,8-catechol as a substrate. B[*a*]P-7,8-dione was reduced to B[*a*]P-7,8-catechol by dithiothreitol under anaerobic conditions and then further glucuronidated by the UGTs in the presence of uridine-5′-diphosphoglucuronic acid as a glucuronic acid group donor. UGT1A1 catalyzed the glucuronidation of B[*a*]P-7,8-catechol and generated two isomeric *O*-monoglucuronsyl-B[*a*]P-7,8-catechol products that were identified by RP-HPLC and by LC-MS/MS. By contrast, UGT1A3 and 2B7 catalyzed the formation of only one monoglucuronide, which was identical to that formed in A549 cells. The kinetic profiles of three UGTs followed Michaelis−Menten kinetics. On the basis of the expression levels of UGT1A3 and UGT2B7 and the observation that a single monoglucuronide was produced in A549 cells, we suggest that the major UGT isoforms in A549 cells that can intercept B[*a*]P-7,8-catechol are UGT1A3 and 2B7.

INTRODUCTION

Polycyclic aromatic hydrocarbons (PAHs) are characterized by the presence of two or more fused benzene rings arranged in various configurations.[1] PAHs are ubiquitous airborne environmental pollutants that arise from the incomplete combustion of fossil fuels and are also present in automobile exhaust and first- and secondhand cigarette smoke. PAHs are one of the major classes of carcinogens found in tobacco smoke and are suspect lung carcinogens. Benzo[*a*]pyrene (B[*a*]P), the most studied PAH, has been recently upgraded to a Group 1 "known human carcinogen" by the International Agency for Research on Cancer.[2,3]

PAHs are not biological reactive, and the biotransformation of PAHs to electrophilic metabolites is required to elicit their tumorigenic effects.[4] There are three major routes for PAH activation which include the formation of radical cations,[5] diol epoxides,[4,6] and electrophilic and redox-active *o*-quinones.[7] In the *o*-quinone pathway, AKRs catalyze the oxidation of proximate PAH carcinogens, *trans*-dihydrodiols, to yield ketols which spontaneously rearrange to catechols. PAH catechols are not stable and undergo autooxidation to form PAH *o*-quinones with the concomitant production of reactive oxygen species (ROS) (Figure 1).[8−11] PAH *o*-quinones are electrophilic and highly reactive with endogenous nucleophiles and yield L-cysteine, *N*-acetyl-L-cysteine, and GSH conjugates.[12] Electrophilic PAH *o*-quinones can also form both depurinating DNA adducts *in vitro*[13] and stable covalent DNA adducts *in vitro* and in human lung cells.[14−16] Apart from their electrophilicity, PAH *o*-quinones are also redox active and undergo nonenzymatic or enzymatic reduction to reform catechols at the expense of consuming NADPH. Enzymes that contribute to this redox cycling include NAD(P)(H):quinone oxidoreductase (NQO1), carbonyl reductases (CBR1 and CBR3), and AKRs themselves. Among these three enzymes, the AKRs are the most efficient.[17] ROS produced by redox cycling of the PAH *o*-quinones mediates DNA damage and can lead to 7,8-dihydro-8-oxo-2′deoxyguanosine (8-oxo-dGuo) lesions[18,19] which contribute to G-to-T transversions in *p53*.[20,21] It was found that even nanomolar concentrations of PAH *o*-quinones were able to

Received: July 20, 2013
Published: September 18, 2013

   dx.doi.org/10.1021/tx400268q | *Chem. Res. Toxicol.* 2013, 26, 1570−1578

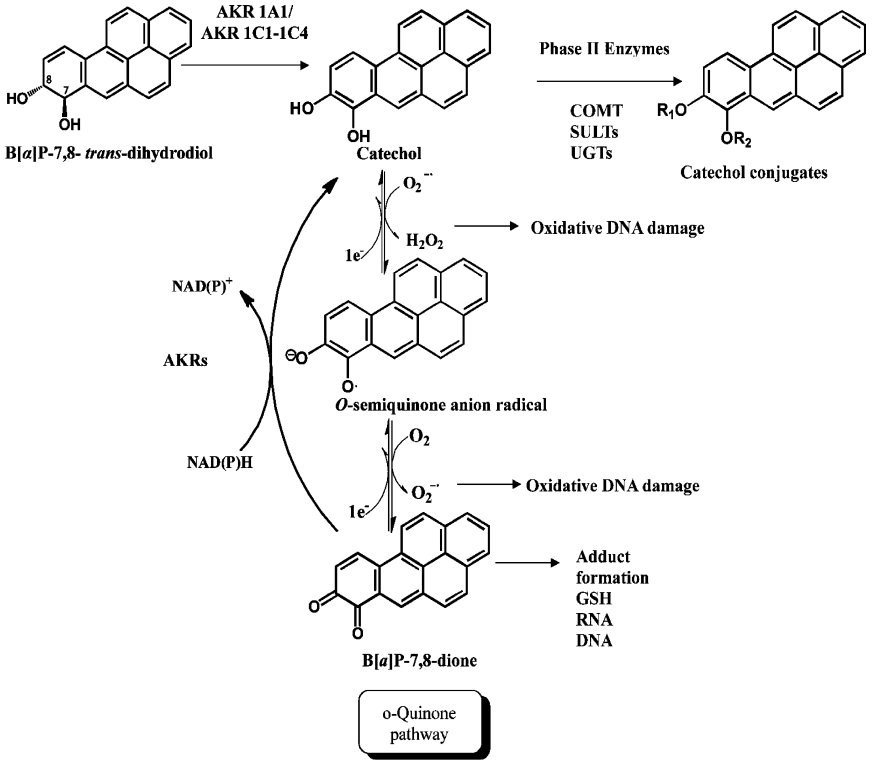

Figure 1. Metabolic activation of B[*a*]P by AKRs and detoxication of B[*a*]P-7,8-dione by UGTs.

generate sufficient ROS to cause a significant increase in 8-oxo-dGuo.[18,19]

Using B[*a*]P as a representative PAH and stable isotope dilution liquid chromatography−tandem mass spectrometry, we found that all three pathways of PAH activation were functional in human bronchoalveolar H358 cells.[22] Also, using A549 cells which show high constitutive expression of AKRs, we found that B[*a*]P-7,8-*trans*-dihydrodiol (an AKR substrate) was converted to B[*a*]P-7,8-dione and that the ROS produced increased the level of 8-oxo-dGuo in cellular DNA as measured by stable isotope dilution liquid chromatography−tandem mass spectrometry.[23] Importantly, the level of 8-oxo-dGuo produced from B[*a*]P-7,8-*trans*-dihydrodiol was elevated further in the presence of a COMT inhibitor suggesting that a redox cycle was occurring.[23]

These observations led to a systematic study of the role of phase II conjugating enzymes in intercepting PAH-catechols to prevent redox cycling. Human catechol-*O*-methyl transferase (COMT) and sulfotransferases (SULT) 1A1, 1A3, and 1E1 were able to detoxify B[*a*]P-7,8-dione by intercepting B[*a*]P-7,8-catechol through the formation of *O*-methylated-B[*a*]P-7,8-catechol and *O*-sulfated-B[*a*]P-7,8-catechol, respectively.[24,25] Another superfamily of phase II metabolic enzymes, uridine diphosphate glucuronosyltransferases (UGTs), are microsomal enzymes which catalyze the transfer of the glucuronosyl group from uridine 5′-diphospho-glucuronic acid (UDPGA) to substrates that contain alcohols, amines, or carboxylic acids as functional groups.[26] UGTs are divided into two main subfamilies UGT1 and UGT2 based on amino acid sequence identity[27] and are responsible for the glucuronidation of a variety of endogenous compounds and xenobiotics.[28] UGTs are widely distributed in a variety of tissues, including the liver, intestine, brain, and kidney, and the aerodigestive tract, etc.[29] UGT1A7, UGT1A8, UGT1A9, and UGT1A10 and UGT2B7 are active against several PAH metabolites,[30−35] while UGT1A10 > UGT1A9 > UGT1A1 > UGT1A7 are the preferred isoforms for catalyzing the glucurondiation of B[*a*]P-7,8-*trans*-dihydrodiol.[36] However, the glucuronidation of PAH catechols by UGTs has not been previously examined.

Studies of B[*a*]P-7,8-dione metabolism and disposition in three human lung cells HBEC-KT, H358, and A549 cells showed rapid disappearance of the quinone accompanied by the formation of phase II conjugates and a N1 or N3-adenine adduct originating from the nucleotide pool.[37] In A549 cells, one of the phase II conjugates was *O*-monoglucuronsyl-B[*a*]P-7,8-catechol indicating that UGTs play a role in the interception/detoxication of PAH catechols. In the present study, we investigated whether glucuronidation catalyzed by human UGTs is a feasible detoxication pathway for B[*a*]P-7,8-dione and identified two major enzyme isoforms responsible for the glucuronidation of B[*a*]P-7,8-catechol.

MATERIALS AND METHODS

Chemical and Reagents. 7-Hydroxy-4-(trifluoromethyl)-coumarin(HFC), alamethicin, and uridine-5′-diphosphoglucuronic acid (UDPGA) were purchased from Sigma-Aldrich Co. (St. Louis, MO). [^{14}C]-Uridine-5′diphosphoglucuronic acid (180 mCi/mmol) was purchased from Perkin Elmer Inc. (Waltham, MA). Benzo[*a*]-pyrene-7,8-dione (B[*a*]P-7,8-dione) was synthesized according to published procedures.[38] All solvents were of HPLC grade, and all other chemicals used were of the highest grade available. UGT1A1, 1A3, and 2B7 Supersomes (microsomes from baculovirus infected insect cells expressing UGTs) were obtained from BD Biosciences (San Jose, CA) and titered before use, using standard substrates.

Cell Lines and Culture Condition. A549 cells (human lung adenocarcinoma cells) were from American Type Culture Collection (ATCC number CCL-185) and cultured in F-12K medium (Kaighn's modification) with supplementation of 10% heat-inactivated FBS, 2 mM L-glutamine, 100 units/mL penicillin, and 100 μg/mL streptomycin. HepG2 cells (hepatoma cells) from ATCC were

Table 1. RT-PCR Primers for UGT Genes Tested in Various Human Cell Lines

genes	forward primers	reverse primers[a,b]	GenBank accession no.	location of forward primer (nt)	length of products (bp)
UGT1A1	5′-AACAAGGAGCTCATGGCCTCC-3′	5′-GTTCGCAAGATTCGATGGTCG-3′	NM_00463	412−432	646
UGT1A3	5′-TGTTGAACAATATGTCTTTGGTCTA-3′	5′-GTTCGCAAGATTCGATGGTCG-3′	NM_019093	347−371	698
UGT1A7	5-ATGCTCGCTGGACGGCACCATTG-3′	5′-GTTCGCAAGATTCGATGGTCG-3′	U89507	284−306	749
UGT1A8	5′-GGTCTTCGCCAGGGGAATAGG-3′	5′-GTTCGCAAGATTCGATGGTCG-3′	AF030310	489−518	535
UGT1A9	5′-GGAGGAACATTTATTATGCCACCG-3′	5′-GTTCGCAAGATTCGATGGTCG-3′	AF056188	660−683	391
UGT1A10	5′-CCTCTTTCCTATGTCCCCAATGA-3′	5′-GTTCGCAAGATTCGATGGTCG-3′	U89508	556−578	477
UGT2B7	5′-TTCACAAGTACAGGAAATCATGTCA-3′	5′-ACCACAACACCATTTTCTCC-3′	NM-001074	341−365	592
β-actin	5′-CACCCACACTGTGCCCATC-3′	5′-CTAGAAGCATTTGCGGTGG-3′			652

[a]The reverse primer for the amplification of UGT2B7 is located between 931-912 nts. Primers were taken from ref 29. [b]The same exon-3 derived antisense primer was used for all RT-PCR amplification of family 1 UGTs.

cultured in Eagle's minimal essential medium supplemented with 10% heat-inactivated fetal bovine serum, 1% L-glutamine, and 100 units/mL penicillin/streptomycin solution. H358 cells (human bronchoalveolar cells) were purchased from American Type Culture Collection (ATCC number CRL-5807) and cultured in RPMI 1640 medium containing 10% heat-inactivated FBS, 2 mM L-glutamine, 100 units/mL penicillin, and 100 μg/mL streptomycin. HBEC-KT cells (immortalized human bronchial epithelial cells) originating from a patient without lung cancer were kindly provided as a gift by Dr. John Minna at University of Texas Southwestern Medical Center and cultured in keratinocyte-serum-free medium with 0.1−0.2 ng/mL recombinant EGF, 20−30 μg/mL bovine pituitary extract, and 2 mM L-glutamine. BEAS-2B cells (normal human bronchial epithelium cells) were obtained from American Type Culture Collection (ATCC number CRL-9609) and cultured in BEGM bronchial epithelium medium (Cambrex CC-3170). Cells were maintained at 37 °C in a humidified atmosphere containing 5% CO_2 and 95% O_2. Cultured cells used in the experiments were confined to passage numbers of 10−20.

RT-PCR Analysis of UGT mRNA Expression in Human Cells. Extraction of total RNA from each cell line was conducted using the RNeasy Kit (Qiagen, Valencia, CA). Reverse transcription (RT) was conducted by using GeneAmp RNA PCR Core Kit according to the manufacturer's protocol (Applied Biosystems, Carlsbad, CA). An aliquot of 1 μL of cDNA synthesized in the above RT reaction was used for PCR. The PCR system (25 μL) contained 1× PCR buffer (10 mM Tris-HCl buffer, pH 8.3, and 50 mM KCl), 2.5 mM $MgCl_2$, 250 μM dNTPs, 0.2 μM primers, and 0.5 U of Taq DNA polymerase (Applied Biosystems, Carlsbad, CA). The sequences of the forward and reverse primer pairs for the amplification of UGT1A1, 1A3, 1A7, 1A8, 1A9, 1A10, and 2B7 and β-actin transcripts are shown in Table 1.[39−41] PCR amplification was performed with a MyCycler Thermal Cycler PCR system (Bio-Rad, CA) using the following protocol. After an initial denaturation step at 94 °C for 3 min, amplification was conducted by denaturation at 95 °C for 30 s, annealing at 61 °C (for UGT1A1), 63 °C (for UGT1A8), or 57 °C (for other UGT isoforms) for 30 s, and extension at 72 °C for 45 s for 35 cycles. The final extension reaction was performed at 72 °C for 7 min. H_2O was used as the negative control. The control samples were amplified using the same conditions as those described above. An aliquot of 20 μL of PCR products was analyzed by electrophoresis in 2% agarose gel with ethidium bromide and visualized under UV light.

Standard Assay for UGT Activity. UGT enzyme assays were conducted as recommended by BD Biosciences (San Jose, CA). Briefly, the reaction system was composed of 50 mM Tris buffer of pH 7.4, 10 mM $MgCl_2$, 1 mM UDPGA, 0.025 mg/mL alamethicin, 50 μM 7-hydroxy-4-(trifluoromethyl)coumarin, and 10 μg of UGT supersome in a final volume of 100 μL. Reactions were initiated by the addition of UDPGA. After incubation at 37 °C for 15 min, the reactions were terminated by the addition of 50 μL of 94% acetonitrile/6% glacial acetic acid and were centrifugated at 16,000g for 10 min. An aliquot of 100 μL of supernatant was carefully pipetted, and 50 μL was injected into HPLC/PDA for the quantification of 7-hydroxy-4-(trifluoromethyl)coumarin glucuronide. The reversed-phase column (Agilent Zorbax-ODS C18, 5 μm, 4.6 × 250 mm, CA) was used for the separation of substrate from product. Elution conditions used a flow rate of 1 mL/min with 80%:20% water/methanol (v/v) containing 0.1% formic acid. The methanol concentration was increased from 20% to 80% over 3 min and kept at 80% methanol for 4 min, then changed back to 20% methanol in 1 min followed by a re-equilibration phase of 7 min at 20% methanol.

Kinetic Studies on Glucuronidation of B[*a*]P-7,8-Catechol. The reactions were performed anaerobically in a glovebox purged with argon. All of the solvent and aqueous solutions were degassed by freeze−pump−thaw cycling five times and stored in sealed containers filled with argon. The experiments were conducted in 1.5 mL amber glass vials with polytetrafluoroethylene/silicone septa closures. The reaction system was composed of 10 mM KPO_4 buffer at pH 7.4, 1.0 mM dithiothreitol, 5.0 mM $MgCl_2$, 0.025 mg/ml alamethicin, 1 mM [^{14}C]-UDPGA (4 dpm/pmol), 0−20 μM B[a]P-7,8-dione, and 15−30 μg of microsomes containing human recombinant UGTs in a final volume of 0.2 mL. The reactions were initiated by the addition of UDPGA and incubated for 30 min (for UGT 1A1) or 60 min (for UGT 1A3 and 2B7) at 25 °C. The incubation time and amount of enzyme used were always in the linear range as determined by plots of initial velocity versus incubation time or enzyme concentration. The reactions were terminated by the addition of 50 μL of ice-cold 1% formic acid and were chilled on ice. The reaction mixtures were extracted with 0.5 mL aliquots of ethyl acetate twice by vortex mixing and centrifuged at 16,000g to help phase separation. The combined ethyl acetate layer was backwashed with 0.2 mL of 1% formic acid by vigorous vortexing and centrifuged at 16,000g. The ethyl acetate was then dried by a SpeedVac concentrator (Thermo Scientific). The residue was dissolved in 100 μL of methanol and analyzed by scintillation counting or by HPLC analysis. Kinetic analyses using nonlinear regression were performed by fitting the Michaelis−Menten equation to the data with the program Grafit,

$$v = V_{max} \times [S]/(K_m + [S])$$

where v is the initial velocity of the reaction, [S] is the molar concentration of the substrate, and K_m is the Michaelis−Menten constant for the substrate. Because of the iterative fits of the equations to each data set, each fit provided estimates of the kinetic parameters as a mean ± SE. Because it is not possible to normalize V_{max} values to UGT protein expression, V_{max} values are apparent values only based on total protein.

Metabolism of B[*a*]P-7,8-Dione in Human Lung Cells. B[a]P-7,8-Dione was prepared in HBSS buffer containing 1 mM sodium pyruvate at final concentration of 2 μM with 0.2% DMSO and then was used to treat A549, HBEC-KT, and H358 cells (5 × 10^6) at confluency. The media were collected at 0 and 24 h and acidified subsequently with 0.1% formic acid before extraction with 2 × 1.5-fold volume of cold H_2O-saturated ethyl acetate. The organic phases of ethyl acetate were combined and dried by a SpeedVac concentrator (Thermo Scientific). The residue was dissolved in 100 μL of methanol. A 20 μL aliquot was analyzed by LC-MS/MS.

Identification of B[*a*]P-7,8-Catechol Glucuronides by HPLC-RAM-UV and LC-MS/MS. The *O*-glucuronsyl-B[*a*]P-7,8-catechol conjugates formed in UGT reaction systems were analyzed by a Waters Alliance 2695 chromatographic system (Waters Corp., Milford, MA) in tandem with a Waters 996 photodiode array detector and a *β*-RAM inline radiometric detector (IN/US Systems Inc., Tampa, FL) or with a Finnigan TSQ Quantum Ultra spectrometer (Thermo Fisher, San Jose, CA). Chromatographic separation was conducted on a reverse-phase column (Agilent Zorbax-ODS C18, 5 μm, 4.6 × 250 mm, CA). The C18 reverse-phase column was eluted with the following linear gradient of H_2O (0.1% formic acid; solvent A)/MeOH (solvent B) at a flow rate of 0.5 mL/min. Solvent B was changed from 50 to 95% (v/v) over 15 min, kept at 95% over 10 min, changed from 95 to 50% over 1 min, and kept at 50% for equilibration for 4 min. The *O*-glucuronsyl-B[*a*]P-7,8-catechols formed in reactions with [^{14}C]-UDPGA were eluted from the C18 reverse-phase column and introduced into the inline radiometric detector using a mixture of the scintillant with the HPLC effluent at a flow rate 1.5 mL/min. The *O*-glucuronsyl-B[*a*]P-7,8-catechols generated with unlabeled UDPGA were eluted from the C18 reverse-phase column and analyzed by electrospray ionization MS/MS. The mass spectrometer analysis was carried out in the positive or negative ion mode with the following parameters: spray voltage (4500 V at positive ion mode or −2000 V at negative ion mode), vaporizer temperature (400 °C), sheath gas pressure (35 arbitrary units), auxiliary gas pressure (10 arbitrary units), capillary temperature (350 °C), and collision energy (20 V). The molecular masses of the metabolites were acquired by detecting the molecular ion from Q1 full scan, and the corresponding mass spectrum of each metabolite was obtained from a Q3 full scan of the product ions of the molecular ions.

RESULTS

Gene Expression of UGTs in Human Lung Cells. We performed RT-PCR to identify the UGT isoforms expressed in HepG2 cells and four human lung cells. The UGTs selected were those that have been previously characterized for the glucuronidation of B[*a*]P-7,8-*trans*-dihydrdodiol (UGT1A10 > UGT1A9 > UGT1A1 > UGT1A7)[36] and the catechol estrogens (UGT1A8, UGT1A9, and UGT2B7).[42] Although RT-PCR is a semiquantitative approach to analyze gene expression, we found that UGT1A1, 1A3, and 2B7 were expressed at the mRNA level in HepG2 and A549 cells among the seven different UGT isoforms examined (Figure 2). The current studies focused on the glucuronidation of B[*a*]P-7,8-catechol by recombinant human UGT1A1, 1A3, and 2B7, which were major UGT isoforms in A549 cells.

Identification of B[*a*]P-7,8-Catechol Glucuronides Produced by Human Recombinant UGT microsomes. Supersomes (BD-Biosciences) containing overexpressed human recombinant UGTs were tittered in standard assays. The standard assay for UGT activity using 7-hydroxy-4-(trifluoromethyl)coumarin as a substrate demonstrated that the specific activities of UGT1A1, 1A3, and 2B7 were 1.18 (0.8), 0.96 (0.7), and 1.74 (1.51) nmol of 7-hydroxy-4-(trifluoromethyl)coumarin glucuronide formed/min/mg, respectively, which are comparable to those values previously reported as indicated by the values in parentheses.[43] UGT1A1, 1A3, and 2B7 were all able to catalyze the glucuronidation of B[*a*]P-7,8-catechol in the presence of UDPGA (Figure 3A,B,C), while no conjugates were generated in the absence of UDPGA (Figure 3D). UGT1A3 and 2B7 catalyzed the formation of one *O*-glucurosonyl-B[*a*]P-7,8-catechol (M2), while UGT1A1 catalyzed the formation of two *O*-glucuronsyl-B[*a*]P-7,8-catechols (M1, M2). The UV spectra of the two glucuronides of B[*a*]P-7,8-catechol (M1, M2) were quite different (Figure 4). When they were compared with the UV

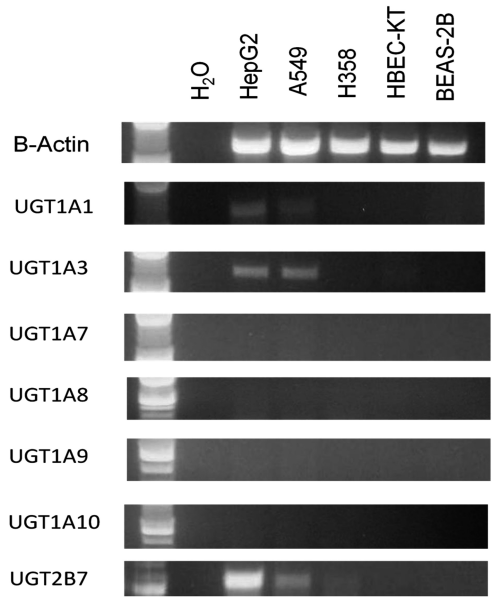

Figure 2. Gene expression of UGTs in various human cell lines. (HepG2, hepatoma cells; A549, human lung adenocarcinoma cells; H358, human bronchoalveolar cells; HBEC-KT, immortalized human bronchial epithelial cells; BEAS-2B, normal human bronchial epithelial cells.)

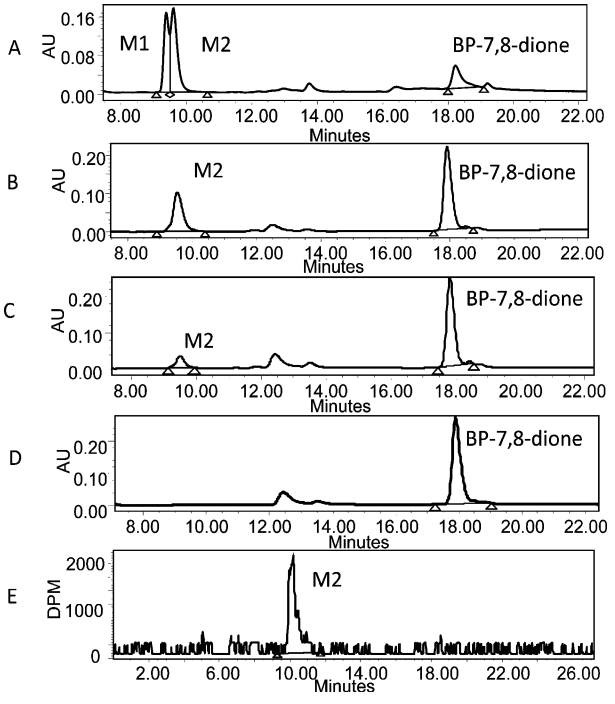

Figure 3. HPLC/UV/RAM identification of B[*a*]P-7,8-catechol glucuronide metabolites (M1 and M2). B[*a*]P-7,8-catechol (20 μM) was generated *in situ* under anaerobic conditions in an incubation buffer containing 1 mM dithiothreitol. B[*a*]P-7,8-catechol was converted to the *O*-glucuronide(s) by UGT Supersomes supplemented with UDPGA (A, UGT1A1; B, UGT1A3; and C, UGT2B7) in the presence of UDPGA. (D) Control incubations were conducted in the absence of UDPGA. (E) HPLC-RAM chromatogram of *O*-monoglucuronsyl-B[*a*]P-7,8-catechol formed by UGT1A3 in the presence of [^{14}C]-UDPGA. The delayed retention time of the M2 metabolite is due to the fact that the radiometeric detector is in-line and downstream from the absorbance (PDA) detector.

dx.doi.org/10.1021/tx400268q | *Chem. Res. Toxicol.* 2013, 26, 1570−1578

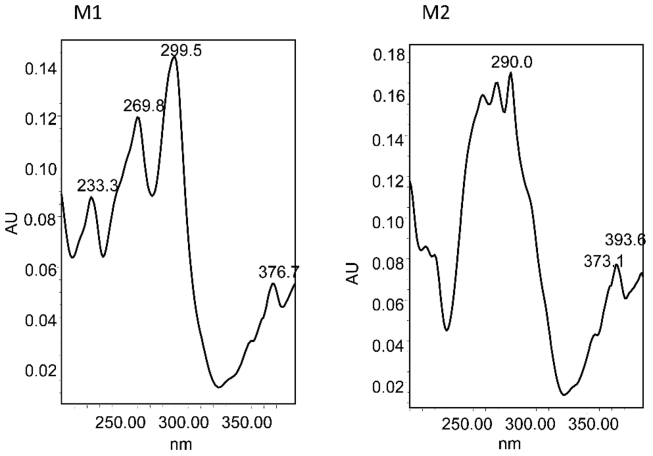

Figure 4. UV spectra of *O*-monoglucuronsyl-B[*a*]P-7,8-catechol metabolites (M1 and M2). B[*a*]P-7,8-catechol (20 μM) was generated *in situ* under anaerobic conditions in an incubation buffer containing 1 mM dithiothreitol. B[*a*]P-7,8-catechol was converted to *O*-glucuronide(s) by UGT1A1 plus UDPGA. UV spectra of M1 and M2 were collected by an in-line Waters 996 photodiode array detector.

spectrum of the *O*-glucuronsyl-B[*a*]P-7,8-catechol found in A549 cell culture media, M2 was identified as the major glucuronide formed in these cells.[37] The formation of glucuronides of B[*a*]P-7,8-catechol was confirmed by conducting the glucuronidation studies in the presence of [^{14}C]-UDPGA. [^{14}C]-*O*-glucuronsyl-B[*a*]P-7,8-catechol was detected with HPLC-RAM analysis (Figure 3 E).

To determine whether B[*a*]-7,8-catechol formed mono- or bis-glucuronide conjugates, LC-MS/MS was used to further characterize the structure the M1 and M2 metabolites. The molecular ions of both metabolites (M1, M2) were the same and showed a ($[M + H]^+$) m/z = 461 in the positive ion mode and a ($[M - H]^-$) m/z = 459 in the negative ion mode, respectively, indicating that both M1 and M2 are *O*-monoglucuronsyl-B[*a*]P-7,8-catechols where the position of glucuronidation is different. MS/MS analysis provided further evidence to the identity of the metabolites. In the positive ion mode, the product ions of the two metabolites were identical, and characteristic scission under collision-induced dissociation occurred at the C−O glycosidic bond with the loss of 176 amu resulting from the loss of the monodehydrated glucuronic acid moiety to yield a fragment ion m/z = 285. Cleavage at one of the C−OH bonds resulted in a daughter ion of m/z = 267 representing the loss of H_2O. Rearrangement resulting in a change of the remaining phenolic group from a −C−OH to −C═O bond is followed by the loss of −C═O group which resulted in a fragment ion at m/z = 239. In the negative ion mode, product ion spectra of two metabolites also demonstrated characteristic cleavage at the C−O glycosidic bond with a loss of 176 amu resulting in daughter ions at m/z = 283. LC-MS/MS analyses in both the positive and negative ion modes confirmed that the metabolites (M1 and M2) formed in the reaction system were *O*-monoglucuronsyl-B[*a*]P-7,8-catechols. Since the mass spectra of M1 and M2 were identical (Figure 5), it was not possible to distinguish the position of glucuronic acid conjugation in the two isomers. However, our studies on the sulfonation of B[*a*]P-7,8-catechol catalyzed by SULTs also led to the formation of two regioisomeric *O*-monosulfated catechols, where the earlier eluting species was shown by 2D-NMR to be the *O*7-monosulfate.[25] Thus, in this study the later eluting M2 metabolite is tentatively assigned as the *O*8-monoglucuronsyl-B[*a*]P-7,8-catechol. LC-MS/MS in the selected reaction monitoring mode (SRM) further confirmed that UGT1A1 catalyzed the formation of isomeric *O*-monoglucuronsyl-B[*a*]P-7,8-catechols (M1, M2) and UGT1A3 and that

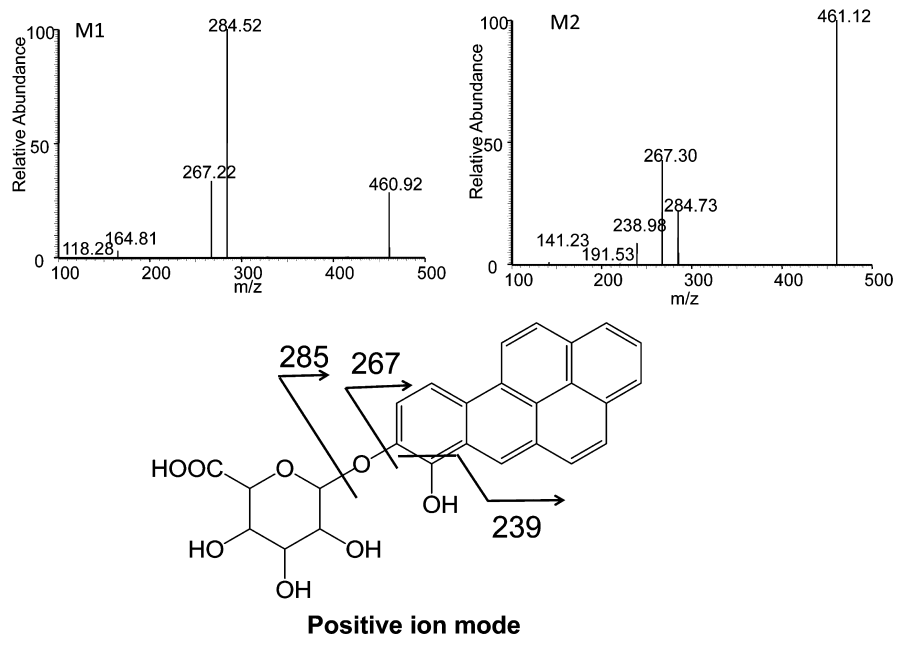

Figure 5. LC/MS/MS identification of *O*-monoglucuronsyl-B[*a*]P-7,8-catechols (M1 and M2). B[*a*]P-7,8-catechol (20 μM) was generated *in situ* under anaerobic conditions in the presence of 1 mM dithiothreitol. B[*a*]P-7,8-catechol was converted to *O*-glucuronide(s) in the presence of UDPGA and UGTs in the incubation buffer. The reaction was quenched by 1% formic acid and extracted with ethyl acetate. The organic phase was then dried and dissolved in MeOH for LC-MS/MS analysis (positive ion mode, MS^2 spectrum of isomer M1 and MS^2 spectrum of isomer M2). The structure of the M2 metabolite is shown.

dx.doi.org/10.1021/tx400268q | *Chem. Res. Toxicol.* 2013, 26, 1570−1578

2B7 catalyzed the formation of only one *O*-monoglucuronsyl-B[*a*]P-7,8-catechol (M2) (Figure 6).

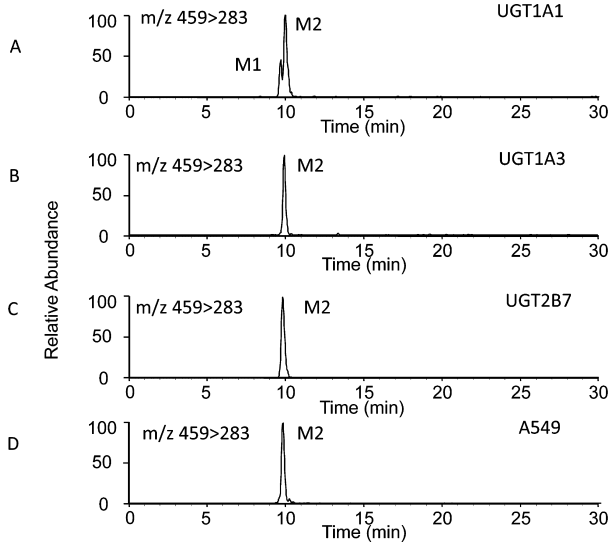

Figure 6. LC-MS/MS detection of *O*-monoglucuronsyl-B[*a*]P-7,8-catechols (M1 and M2) formed by recombinant UGT1A1 (A), 1A3 (B), 2B7 (C), and by A549 (D) at 24 h. B[*a*]P-7,8-catechol (20 μM) was generated *in situ* under anaerobic conditions in the presence of 1 mM dithiothreitol. B[*a*]P-7,8-catechol was converted to the *O*-glucuronide(s) in the presence of UDPGA and UGTs in the incubation buffer (A, UGT1A1; B, UGT1A3; and C, UGT2B7). (D) B[*a*]P-7,8-dione (2 μM, 0.2% DMSO) in HBSS medium was incubated with A549 cells and the culture media collected at 0 and 24 h, respectively. The culture media were acidified by formic acid and extracted with ethyl acetate. The organic phases were dried under vacuum and redissolved in methanol. *O*-Monoglucuronsyl-B[*a*]P-7,8-catechols were analyzed with LC-MS/MS in a negative ion mode by monitoring the mass transition *m/z* 459 → 283 ($[M - H]^- \rightarrow [M - H\text{-glucuronic acid group}]^-$).

Kinetic Studies on Glucuronidation of B[*a*]P-7,8-Catechol. To elucidate the steady state kinetic properties of the recombinant UGTs to glucuronidate B[*a*]P-7,8-catechol, we performed discontinuous assays to monitor the initial velocity of conjugate formation using [^{14}C]-UDPGA as the cofactor. Because of substrate solubility, the substrate concentration was limited to 0−20 μM. B[*a*]P-7,8-Catechol glucuronidation catalyzed by UGT1A1, 1A3, and 2B7 followed Michaelis−Menten kinetics (Figure 7). Apparent utilization ratios (V_{maxapp}/K_m) showed that UGT1A1 Supersomes were the most catalytically efficient for the glucuronidation of B[*a*]P-7,8-catechol, followed by UGT1A3 and 2B7 Supersomes (Table 2). The K_m values of UGT1A1 and 1A3 were 9.6 and 8.5 μM, respectively, which were slightly lower than that of UGT2B7 at 16.3 μM indicating that the substrate concentration at which half maximal velocity was observed was similar in each case.

Glucuronidation of B[*a*]P-7,8-Catechol in Human Lung Cells Treated with 2 μM B[*a*]P-7,8-Dione. Only one *O*8-monoglucuronsyl-B[*a*]P-7,8-catechol (M2) was detected by LC-MS/MS in the SRM mode in A549 cells after incubation of the cells with 2 μM B[*a*]P-7,8-dione for 24 h. By contrast, *O*-monoglucuronsyl-B[*a*]P-7,8-catechol was not detected in H358 and HBEC-KT cell lines, which was consistent with the low mRNA level of UGTs in these cell lines (Figures 2 and 6D).

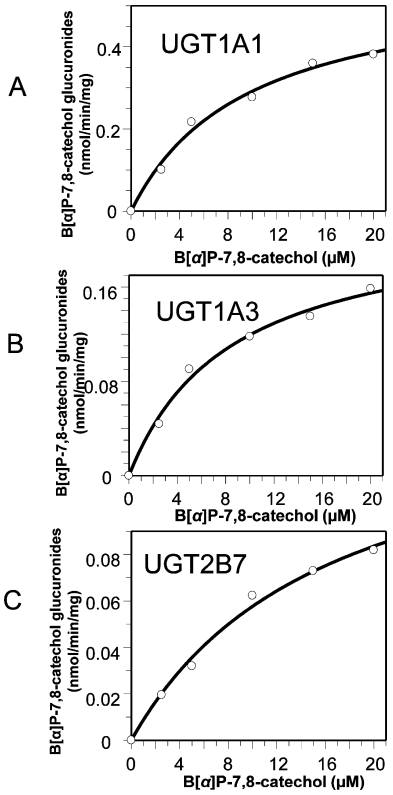

Figure 7. Kinetic characterization of glucuronidation of B[*a*]P-7,8-catechol by UGTs. Kinetic analyses were performed by fitting the Michaelis−Menten equation to the data. Reactions contained 10 mM KPO_4 buffer at pH 7.4, 1.0 mM dithiothreitol, 5.0 mM $MgCl_2$, 1 mM [^{14}C]UDPGA, 0−20 μM B[*a*]P-7,8-dione, and 15−30 μg of human recombinant UGT Supersomes at 25 °C. A, B, and C, velocity versus [S] curve for the glucuronidation of B[*a*]P-7,8-catechol by UGT1A1, 1A3, and 2B7, respectively.

Table 2. Kinetic Constants of Glucuronidation of B[*a*]P-7,8-Catechol

enzymes	V_{max} (μM/min/mg)	K_m (μM)	V_{max}/K_m(min^{-1} mg^{-1})
UGT1A1	2.9 ± 0.25	9.60 ± 1.97	0.3
UGT1A3	1.1 ± 0.1	8.50 ± 1.65	0.12
UGT2B7	0.75 ± 0.1	16.3 ± 3 0.5	0.5

DISCUSSION

We have been conducting a systematic study to elucidate the roles of human enzymes in catalyzing the redox cycling of PAH *o*-quinones and the roles of phase II enzymes in conjugating PAH catechols that arise from the AKR pathway of PAH activation. Previous studies have shown that AKRs are efficient PAH *o*-quinone reductases[17] and that the PAH catechols formed can be intercepted by COMTs and SULTs.[24,25] We now show that UGT1A1, 1A3, and 2B7 are all expressed in A549 cells. Of these, UGT1A3 and 2B7 are the enzymes most likely involved in B[*a*]P-7,8-catechol glucuronidation based on the glucuronide product profile. While recombinant UGT1A1 expressed in Supersomes produces two regioisomeric monoglucuronides with B[*a*]P-7,8-catechol, only one of the isomers is produced in A549 cells and corresponds to the single isomer produced by UGT1A3 and UGT2B7. The monoglucuronide formed is tentatively assigned as *O*8-monoglucuronsyl-B[*a*]P-7,8-catechol based on differences in retention time observed for the regioisomeric *O*-monosulfated B[*a*]P-7,8-catechols.[25]

dx.doi.org/10.1021/tx400268q | *Chem. Res. Toxicol.* 2013, 26, 1570−1578

It is noteworthy that UGT2B7 is also the dominant isoform involved in the glucuronidation of the structurally related catechol estrogens.[42] UGT2B7 catalyzes the glucuronidation of 4-hydroxycatecholestrogens (hydroxylated estrone/estradiol), which are structurally similar to B[*a*]P-7,8-catechol.[44] The glucuronidation of 4-hydroxycatecholestrogens shows preference for the C4-hydroxyl group, which would be equivalent to the C7 position of B[*a*]P-7,8-catechol. Although UGT1A1 was found in the kinetic analysis to have the highest utilization ratio (V_{max}/K_m) and catalyzed the formation of both regioisomeric B[*a*]P-7,8-catechol glucuronides, no significant M1 was found in A549 cells indicating that it did not contribute to the detoxication of this catechol in these cells.

It is noteworthy that only A549 cells expressed the UGT isoforms studied to any extent. The low expression of UGTs might be anticipated due to the low level of expression previously reported in human lung specimens. Zheng at al. measured the expression of multiple UGTs in 32 human lung tissues by duplex RT-PCR and found that UGT1A1, UGT1A3, UGT1A4, UGT1A6, UGT1A7, UGT1A8, UGT1A9, and UGT1A10 were not expressed.[29] Similarly, UGT2B4, UGT2B7, UGT2B15, and UGT2B17 were not detected. In later studies, Dillinger et al. showed that UGT1A10 was found in low amounts in human lung specimens.[45] The difference in UGT isoform expression observed in our study versus that observed in the earlier work could reflect differences in measuring UGT expression in human bronchial epithelial cells versus whole lung tissue. Other UGTs that could have been included in our study would be UGT2B10, but up until now, this has only been shown in glucuronidate tobacco specific nitrosamines.[46]

The formation of regioisomeric *O*-monoglucuronides of B[*a*]P-7,8-catechol also deserves comment. UGT1A1, UGT1A9, and UGT2B7, which are predominately expressed in the liver, were found to form the 7*S*-monoglucuronide from (±)-B[*a*]P-7,8-*trans*-dihydrodiol, whereas the extrahepatic UGT1A7, UGT1A8, and UGT1A10 could form either the 7*R*-monoglucuronide or the 8*S*-monoglucuronide, i.e., they produce two different enantiomers.[36] By contrast, UGT1A1 formed two different regioisomeric B[*a*]P-7,8-catechol monoglucuronides, whereas UGT1A3 and UGT2B7 produced a single regioisomeric *O*-monoglucuronsyl-B[*a*]P-7,8-catechol. The ability of UGTs to form different enantiomers from B[*a*]P-7,8-*trans*-dihydrodiol may be related to the fact that the dihydrodiol is nonplanar and has both axial and equatorial alcohols. By contrast, the catechol is planar, and only different regioisomers are allowed. No bis-glucuronide has been observed with either B[*a*]P-7,8-*trans*-dihydrodiol or B[*a*]P-7,8-catechol possibly due to steric hindrance.

We next compared the specific activities for the redox cycling of B[*a*]P-7,8-dione catalyzed by AKRs, with the specific activities observed for *O*-methylation, *O*-sulfation, and *O*-glucuronidation of B[*a*]P-7,8-catechol catalyzed by COMTs, SULTs, and UGTs in Table 3. These data reveal that the rates of redox cycling are much greater than the rates of phase II conjugating reactions. Although some uncertainties exist in this comparison due to the differences in expression levels of these enzymes in specific cells, it is unlikely that these will account for the >6,000-fold difference in the specific activities of NQO1 and UGT1A3 to use B[*a*]P-7,8-dione and B[*a*]P-7,8-catechol as substrates, respectively. Thus, the ability to intercept the PAH catechols and prevent redox cycling is not an efficient process and could be easily overwhelmed in a cellular environment. This is supported by earlier work in which we showed that B[*a*]P-7,8-*trans*-dihydrodiol (AKR substrate) and B[*a*]P-7,8-dione (AKR product) produced significant ROS and 8-oxo-dGuo formation in A549 cells.[23]

Table 3. Comparison of Rates of PAH *o*-Quinone Redox Cycling with Rates of Phase II Conjugation Reactions[a]

recombinant enzyme	specific activity[b] (nmol/min/mg)
NQO1	1070[c]
AKR7A2	1270[c]
AKR1C1	64[c]
sCOMT	55[d]
SULT1A1	0.8[d]
UGT1A1	0.3[d]
UGT 1A3	0.16[d]
UGT2B7	0.06[d]

[a]The values were taken from refs 17, 24, and 25. [b]Substrate concentration was 10 μM B[*a*]P-7,8-dione. [c]Six replicates with SD < 10%. [d]From Michaelis−Menton plots.

Although UGTs were not detected in HBEC-KT, H358, and BEAS-2B under current culture conditions, the contribution of UGTs in human lung cells to B[*a*]P-7,8-catechol conjugation may be affected by the induction of UGTs. Cigarette smoke increases UGT activity.[47,48] It has been proposed that the expression level of UGT1A4 in the human small airway epithelium was elevated as a result of nuclear factor erythroid 2 p45-related factors (Nrf2) activation. However, UGT1A4 does not appear to be responsible for B[*a*]P-7,8-catechol glucuronidation in our experiments to date.[49] It has also been demonstrated that UGT1A10 and UGT1A8 are coordinately regulated by the aryl hydrocarbon receptor (AhR) and Nrf2 and that the Nrf2 response requires the presence of AhR.[50] Both PAHs and PAH *o*-quinones such as B[*a*]P-7,8-dione are the ligands of the AhR, which is required for the induction of UGTs by Nrf2.[51−53] With the induction of UGTs, the detoxification of B[*a*]P-7,8-dione by UGTs in smokers could become more significant.

The *AKR1C* genes involved in the formation and redox cycling of PAH *o*-quinones are also highly induced by the Nrf2-Keap 1 system.[54,55] Inducers that activate Nrf2 include electrophiles and ROS and not surprisingly PAH *o*-quinones. Thus, the induction of *AKR1C* genes with the products of PAH-*trans*-dihydrodiol oxidation, namely, PAH *o*-quinones, could lead to an exacerbation of ROS formation which may not be easily countered by UGT induction.

AUTHOR INFORMATION

Corresponding Author

*Department of Pharmacology, Perelman School of Medicine, University of Pennsylvania, 1315 Biomedical Research Building II/III, 421 Curie Boulevard, Philadelphia, PA 19104-6160. Phone: 215-898-9445. Fax: 215-573-0200. E-mail: penning@upenn.edu.

Funding

This work was supported by NIH grants P30-ES-013508, R01-CA39504, and PA-DOH4100038714.

Notes

The authors declare no competing financial interest.

■ ACKNOWLEDGMENTS

We thank Drs. Mo Chen, Rebekka Mindnich, and Ms. Ling Duan for suggestions on experimental design. We thank Dr. Xiaojing Liu for the advice on LC/MS method development.

■ ABBREVIATIONS

AKR, aldo-keto reductase; AhR, aryl hydrocarbon receptor; B[*a*]P, benzo[*a*]pyrene; CBR, carbonyl reductase; COMT, catechol-*O*-methyl transferase; 8-oxo-dGuo, 7,8-dihydro-8-oxo-2′-deoxyguanosine; PAH, polycyclic aromatic hydrocarbon; NQO1, NAD(P)(H):quinone oxidoreductase; Nrf2, nuclear factor erythroid 2 p45-related factor; ROS, reactive oxygen species; SULT, sulfotransferase; UDPGA, uridine-5′-diphosphoglucronic acid; UGT, uridine glucuronsyltransferase

■ REFERENCES

(1) Fetzer, J. C. (2007) The chemistry and analysis of large PAH. *Polycyclic Aromat. Compd. 27*, 143−162.

(2) IARC (2010) Some non-heterocyclic polycyclic aromatic hydrocarbons and some related exposures. *IARC Monogr. Eval. Carcinog. Risks Hum. 92*, 754−773.

(3) Straif, K., Baan, R., Grosse, Y., Secretan, B., El Ghissassi, F., and Cogliano, V. (2005) Carcinogenicity of polycyclic aromatic hydrocarbons. *Lancet Oncol. 6*, 931−932.

(4) Gelboin, H. V. (1980) Benzo[alpha]pyrene metabolism, activation and carcinogenesis: role and regulation of mixed-function oxidases and related enzymes. *Physiol. Rev. 60*, 1107−1166.

(5) Cavalieri, E. L., and Rogan, E. G. (1995) Central role of radical cations in the metabolic activation of polycyclic aromatic hydrocarbons. *Xenobiotica 25*, 677−688.

(6) Conney, A. H. (1982) Induction of microsomal enzymes by foreign chemicals and carcinogenesis by polycyclic aromatic hydrocarbons. G.H.A. Clowes Memorial Lecture. *Cancer Res. 42*, 4875−4917.

(7) Penning, T. M., Burczynski, M. E., Hung, C. F., McCoull, K. D., Palackal, N. T., and Tsuruda, L. S. (1999) Dihydrodiol dehydrogenases and polycyclic aromatic hydrocarbon activation: generation of reactive and redox active *o*-quinones. *Chem. Res. Toxicol. 12*, 1−18.

(8) Burczynski, M. E., Harvey, R. G., and Penning, T. M. (1998) Expression and characterization of four recombinant human dihydrodiol dehydrogenase isoforms: oxidation of *trans*-7,8-dihydroxy-7,8-dihydrobenzo[*a*]pyrene to the activated *o*-quinone metabolite benzo[*a*]pyrene-7,8-dione. *Biochemistry 37*, 6781−6790.

(9) Palackal, N. T., Burczynski, M. E., Harvey, R. G., and Penning, T. M. (2001) The ubiquitous aldehyde reductase (AKR1A1) oxidizes proximate carcinogen *trans*-dihydrodiols to *o*-quinones: potential role in polycyclic aromatic hydrocarbon activation. *Biochemistry 40*, 10901−10910.

(10) Palackal, N. T., Lee, S. H., Harvey, R. G., Blair, I. A., and Penning, T. M. (2002) Activation of polycyclic aromatic hydrocarbon *trans*-dihydrodiol proximate carcinogens by human aldo-keto reductase (AKR1C) enzymes and their functional overexpression in human lung carcinoma (A549) cells. *J. Biol. Chem. 277*, 24799−24808.

(11) Penning, T. M., Ohnishi, S. T., Ohnishi, T., and Harvey, R. G. (1996) Generation of reactive oxygen species during the enzymatic oxidation of polycyclic aromatic hydrocarbon *trans*-dihydrodiols catalyzed by dihydrodiol dehydrogenase. *Chem. Res. Toxicol. 9*, 84−92.

(12) Murty, V. S., and Penning, T. M. (1992) Characterization of mercapturic acid and glutathionyl conjugates of benzo[*a*]pyrene-7,8-dione by two-dimensional NMR. *Bioconjugate Chem. 3*, 218−224.

(13) McCoull, K. D., Rindgen, D., Blair, I. A., and Penning, T. M. (1999) Synthesis and characterization of polycyclic aromatic hydrocarbon *o*-quinone depurinating N7-guanine adducts. *Chem. Res. Toxicol. 12*, 237−246.

(14) Balu, N., Padgett, W. T., Lambert, G. R., Swank, A. E., Richard, A. M., and Nesnow, S. (2004) Identification and characterization of novel stable deoxyguanosine and deoxyadenosine adducts of benzo[*a*]pyrene-7,8-quinone from reactions at physiological pH. *Chem. Res. Toxicol. 17*, 827−838.

(15) Huang, M., Blair, I. A., and Penning, T. M. (2013) Identification of stable benzo[*a*]pyrene-7,8-dione-DNA adducts in human lung cells. *Chem. Res. Toxicol. 26*, 685−692.

(16) Shou, M., Harvey, R. G., and Penning, T. M. (1993) Reactivity of benzo[*a*]pyrene-7,8-dione with DNA. Evidence for the formation of deoxyguanosine adducts. *Carcinogenesis 14*, 475−482.

(17) Shultz, C. A., Quinn, A. M., Park, J. H., Harvey, R. G., Bolton, J. L., Maser, E., and Penning, T. M. (2011) Specificity of human aldo-keto reductases, NAD(P)H:quinone oxidoreductase, and carbonyl reductases to redox-cycle polycyclic aromatic hydrocarbon diones and 4-hydroxyequilenin-*o*-quinone. *Chem. Res. Toxicol. 24*, 2153−2166.

(18) Park, J. H., Gopishetty, S., Szewczuk, L. M., Troxel, A. B., Harvey, R. G., and Penning, T. M. (2005) Formation of 8-oxo-7,8-dihydro-2′-deoxyguanosine (8-oxo-dGuo) by PAH *o*-quinones: involvement of reactive oxygen species and copper(II)/copper(I) redox cycling. *Chem. Res. Toxicol. 18*, 1026−1037.

(19) Park, J. H., Troxel, A. B., Harvey, R. G., and Penning, T. M. (2006) Polycyclic aromatic hydrocarbon (PAH) *o*-quinones produced by the aldo-keto-reductases (AKRs) generate abasic sites, oxidized pyrimidines, and 8-oxo-dGuo via reactive oxygen species. *Chem. Res. Toxicol. 19*, 719−728.

(20) Park, J. H., Gelhaus, S., Vedantam, S., Oliva, A. L., Batra, A., Blair, I. A., Troxel, A. B., Field, J., and Penning, T. M. (2008) The pattern of p53 mutations caused by PAH *o*-quinones is driven by 8-oxo-dGuo formation while the spectrum of mutations is determined by biological selection for dominance. *Chem. Res. Toxicol. 21*, 1039−1049.

(21) Shen, Y. M., Troxel, A. B., Vedantam, S., Penning, T. M., and Field, J. (2006) Comparison of p53 mutations induced by PAH *o*-quinones with those caused by *anti*-benzo[a]pyrene diol epoxide *in vitro*: role of reactive oxygen and biological selection. *Chem. Res. Toxicol. 19*, 1441−1450.

(22) Lu, D., Harvey, R. G., Blair, I. A., and Penning, T. M. (2011) Quantitation of benzo[*a*]pyrene metabolic profiles in human bronchoalveolar (H358) cells by stable isotope dilution liquid chromatography-atmospheric pressure chemical ionization mass spectrometry. *Chem. Res. Toxicol. 24*, 1905−1914.

(23) Park, J. H., Mangal, D., Tacka, K. A., Quinn, A. M., Harvey, R. G., Blair, I. A., and Penning, T. M. (2008) Evidence for the aldo-keto reductase pathway of polycyclic aromatic *trans*-dihydrodiol activation in human lung A549 cells. *Proc. Natl. Acad. Sci. U.S.A. 105*, 6846−6851.

(24) Zhang, L., Jin, Y., Chen, M., Huang, M., Harvey, R. G., Blair, I. A., and Penning, T. M. (2011) Detoxication of structurally diverse polycyclic aromatic hydrocarbon (PAH) *o*-quinones by human recombinant catechol-*O*-methyltransferase (COMT) via *O*-methylation of PAH catechols. *J. Biol. Chem. 286*, 25644−25654.

(25) Zhang, L., Huang, M., Blair, I. A., and Penning, T. M. (2012) Detoxication of benzo[*a*]pyrene-7,8-dione by sulfotransferases (SULTs) in human lung cells. *J. Biol. Chem. 287*, 29909−29920.

(26) Bock, K. W., and Kohle, C. (2005) UDP-glucuronosyltransferase 1A6: structural, functional, and regulatory aspects. *Methods Enzymol. 400*, 57−75.

(27) Tukey, R. H., and Strassburg, C. P. (2000) Human UDP-glucuronosyltransferases: metabolism, expression, and disease. *Annu. Rev. Pharmacol. Toxicol. 40*, 581−616.

(28) King, C. D., Rios, G. R., Green, M. D., and Tephly, T. R. (2000) UDP-glucuronosyltransferases. *Curr. Drug Metab. 1*, 143−161.

(29) Zheng, Z., Fang, J.-L., and Lazarus, P. (2002) Glucuronidation: An important mechanism for detoxication of benzo[*a*]pyrene metabolites in aerodigestive tract tissues. *Drug Metab. Dispos. 30*, 397−403.

(30) Grove, A. D., Kessler, F. K., Metz, R. P., and Ritter, J. K. (1997) Identification of a rat olitpratz-inucible UDP-glucuronsyltransferase (UGT1A7) with activity towards benzo[*a*]pyrene-7,8-dihydrodiol. *J. Biol. Chem. 272*, 1621−1627.

(31) Guillemette, C., Ritter, J. K., Auyeung, D. J., Kessler, F. K., and Housman, D. E. (2000) Structural heterogeneity at the UDP-

glucuronosyltransferase 1 locus: functional consequences of three novel missense mutations in the human UGT1A7 gene. *Pharmacogenetics 10*, 629−644.
(32) Jin, C. J., Miners, J. O., Burchell, B., and MacKenzie, P. I. (1993) The glucurondiation of hydroxylated metabolites of benzo[*a*]pyrene and 2-acetyl-aminoflluorene by cDNA-expressed human UDP-glucuronsyltransferases. *Carcinogenesis 14*, 2637−2639.
(33) Jin, C. J., Miners, J. O., Lillywhite, K. J., and Mackenzie, P. I. (1993) cDNA cloning and expression of two new members of the human liver glucuronsyltransferase 2B subfamily. *Biochem. Biophys. Res. Commun. 194*, 496−503.
(34) Mojarrabi, B., and Mackenzie, P. I. (1998) Characterization of two UDP glucuronsyltransferases that are predominately expressed in human colon. *Biochem. Biophys. Res. Commun. 246*, 704−709.
(35) Strassburg, C. P., Strassburg, A., Nguyen, N., Li, Q., Mann, M. P., and Tukey, R. H. (1999) Regulation and function of family 1 and family 2 UDP-glucuronsyltransferase genes (UGT1A, UGT2B) in human oesophagus. *Biochem. J. 338*, 489−498.
(36) Fang, J., Beland, F. A., Doerge, D. R., Wiener, D., Guillemette, C., Marques, M. M., and Lazarus, P. (2002) Characterization of benzo(a)pyrene-*trans*-7,8-dihydrodiol glucuronidation by human tissue microsomes and overexpressed UDP-glucuronosyltransferase enzymes. *Cancer Res. 62*, 1978−1986.
(37) Huang, M., Liu, X., Basu, S., Zhang, L., Kushman, M., Harvey, R. G., Blair, I. A., and Penning, T. M. (2012) Metabolism and disposition of benzo[a]pyrene-7,8-dione (B[*a*]P-7,8-dione) in human lung cells by liquid chromatography tandem mass spectrometry: Detection of an adenine B[*a*]P-7,8-dione adduct. *Chem. Res. Toxicol. 25*, 993−1003.
(38) Harvey, R. G., Dai, Q., Ran, C., and Penning, T. M. (2004) Synthesis of the *o*-quinones and other oxidized metabolites of polycyclic aromatic hydrocarbons implicated in carcinogenesis. *J. Org. Chem. 69*, 2024−2032.
(39) Zheng, Z., Park, J. Y., Guillemette, C., Schantz, S. P., and Lazarus, P. (2001) Tobacco carcinogen-detoxifying enzyme UGT1A7 and its association with orolaryngeal cancer risk. *J. Natl. Cancer Inst. 93*, 1411−1418.
(40) Strassburg, C. P., Oldhafer, K., Manns, M. P., and Tukey, R. H. (1997) Differential expression of the UGT1A locus in human liver, biliary, and gastric tissue: identification of UGT1A7 and UGT1A10 transcripts in extrahepatic tissue. *Mol. Pharmacol. 52*, 212−220.
(41) Stanley, E. L., Hume, R., and Coughtrie, M. W. (2005) Expression profiling of human fetal cytosolic sulfotransferases involved in steroid and thyroid hormone metabolism and in detoxification. *Mol. Cell. Endocrinol. 240*, 32−42.
(42) Thibaudeau, J., Lépine, J., Tojcic, J., Duguay, Y., Pelletier, G., Plante, M., Brisson, J., Têtu, B., Jacob, S., Perusse, L., Bélanger, A., and Guillemette, C. (2006) Characterization of common UGT1A8, UGT1A9, and UGT2B7 variants with different capacities to inactivate mutagenic 4-hydroxylated metabolites of estradiol and estrone. *Cancer Res. 66*, 125−133.
(43) Boersma, M. G., van der Woude, H., Bogaards, J., Boeren, S., Vervoort, J., Cnubben, N. H., van Iersel, M. L., van Bladeren, P. J., and Rietjens, I. M. (2002) Regioselectivity of phase II metabolism of luteolin and quercetin by UDP-glucuronosyl transferases. *Chem. Res. Toxicol. 15*, 662−670.
(44) Lepine, J., Bernard, O., Plante, M., Tetu, B., Pelletier, G., Labrie, F., Belanger, A., and Guillemette, C. (2004) Specificity and regioselectivity of the conjugation of estradiol, estrone, and their catecholestrogen and methoxyestrogen metabolites by human uridine diphospho-glucuronosyltransferases expressed in endometrium. *J. Clin. Endocrinol. Metab. 89*, 5222−5232.
(45) Dellinger, R. W., Fang, J.-L., Chen, G., Weiberg, R., and Lazarus, P. (2006) Importance of UDP-glucuronsyltransferase 1A10 (UGT1A10) in the detoxification of polycyclic aromatic hydrocarbons: decresaed glucuronidative activity of the UGT1A10^{139Lys} isoform. *Drug Metab. Dispos. 34*, 943−949.
(46) Chen, G., Dellinger, R. W., Sun, D., Spratt, T. E., and Lazarus, P. (2008) Glucuronidation of tobacco-specific nitrosamines by UGT2B10. *Drug Metab. Dispos. 36*, 824−830.
(47) Bock, K. W., Schrenk, D., Forster, A., Griese, E. U., Morike, K., Brockmeier, D., and Eichelbaum, M. (1994) The influence of environmental and genetic factors on CYP2D6, CYP1A2 and UDP-glucuronosyltransferases in man using sparteine, caffeine, and paracetamol as probes. *Pharmacogenetics 4*, 209−218.
(48) Villard, P. H., Herber, R., Seree, E. M., Attolini, L., Magdalou, J., and Lacarelle, B. (1998) Effect of cigarette smoke on UDP-glucuronosyltransferase activity and cytochrome P450 content in liver, lung and kidney microsomes in mice. *Pharmacol. Toxicol. 82*, 74−79.
(49) Hubner, R. H., Schwartz, J. D., De Bishnu, P., Ferris, B., Omberg, L., Mezey, J. G., Hackett, N. R., and Crystal, R. G. (2009) Coordinate control of expression of Nrf2-modulated genes in the human small airway epithelium is highly responsive to cigarette smoking. *Mol. Med. 15*, 203−219.
(50) Kalthoff, S., Ehmer, U., Freiberg, N., Manns, M. P., and Strassburg, C. P. (2010) Interaction between oxidative stress sensor Nrf2 and xenobiotic-activated aryl hydrocarbon receptor in the regulation of the human phase II detoxifying UDP-glucuronosyltransferase 1A10. *J. Biol. Chem. 285*, 5993−6002.
(51) Okey, A. B., Riddick, D. S., and Harper, P. A. (1994) Molecular biology of the aromatic hydrocarbon (dioxin) receptor. *Trends Pharmacol. Sci. 15*, 226−232.
(52) Burczynski, M. E., and Penning, T. M. (2000) Genotoxic polycyclic aromatic hydrocarbon *ortho*-quinones generated by aldo-keto reductases induce *CYP1A1* via nuclear translocation of the aryl hydrocarbon receptor. *Cancer Res. 60*, 908−915.
(53) Park, J. H., Mangal, D., Frey, A. J., Harvey, R. G., Blair, I. A., and Penning, T. M. (2009) Aryl hydrocarbon receptor facilitates DNA strand breaks and 8-oxo-2′-deoxyguanosine formation by the aldo-keto reductase product benzo[*a*]pyrene-7,8-dione. *J. Biol. Chem. 284*, 29725−29734.
(54) Burczynski, M. E., Lin, H.-K., and Penning, T. M. (1999) Isoform-specific induction of a human aldo-keto reductase by polycyclic aromatic hydrocarbons (PAHs), electrophiles, and oxidative stress: implications for the alternative pathway of PAH activation catalyzed by human dihydrodiol dehydrogenases. *Cancer Res. 59*, 607−614.
(55) Lou, H., Du, S., Ji, Q., and Stolz, A. (2006) Induction of AKR1C2 by phase II inducers: identification of a distal consensus antioxidant response element (ARE) regulated by Nrf2. *Mol. Pharmacol. 69*, 1662−1672.